Journal of Parasitology 2019 105(5) 704–717

Published 4 October 2019

DOI: 10.1645/19-61

Contents and archives available through www.bioone.org or www.jstor.org

Journal of Parasitology

journal homepage: www.journalofparasitology.org

PHYLOGENETIC AFFINITIES OF *UVULIFER* SPP. (DIGENEA: DIPLOSTOMIDAE) IN THE AMERICAS WITH DESCRIPTION OF TWO NEW SPECIES FROM PERUVIAN AMAZON

Tyler J. Achatz[1], Stephen S. Curran[2], Kaylyn F. Patitucci[1], Alan Fecchio[3], and Vasyl V. Tkach[1]

[1] Department of Biology, University of North Dakota, Starcher Hall, 10 Cornell Street Stop 9019, Grand Forks, North Dakota 58202.
[2] Division of Coastal Sciences, University of Southern Mississippi, 703 East Beach Drive, Ocean Springs, Mississippi 39564.
[3] Programa de Pós-Graduação em Ecologia e Conservação da Biodiversidade, Universidade Federal de Mato Grosso, Cuiabá, MT 78060900, Brazil.
Correspondence should be sent to V. V. Tkach at: *vasyl.tkach@und.edu*

KEY WORDS

Diplostomidae
Molecular Phylogeny
Uvulifer batesi n. sp.
Uvulifer pequenae n. sp.
Uvulifer ambloplitis
Chloroceryle inda
Kingfishers
Amazon
Peru
Brazil

ABSTRACT

Uvulifer Yamaguti, 1934, is a genus of diplostomoidean digeneans that parasitizes kingfishers worldwide. Species have a *Neascus*-type metacercaria that encysts in or on fish intermediate hosts, often causing black spot disease. Only 3 prior studies published DNA sequence data for *Uvulifer* species with only 1 including a single named species (*Uvulifer spinatus* López-Jiménez, Pérez-Ponce de León, & García-Varela, 2018). Herein we describe 2 new species of *Uvulifer* from the green-and-rufous kingfisher, *Chloroceryle inda* (Linnaeus), collected in Peru (*Uvulifer batesi* n. sp. and *Uvulifer pequenae* n. sp.). Both new species are readily differentiated from their New World congeners by a combination of morphological characters including distribution of vitelline follicles and prosoma:opisthosoma length ratios. In addition, we used newly generated nuclear *28S rRNA* and mitochondrial *COI* gene sequence data to differentiate among species and examine phylogenetic affinities of *Uvulifer*. This includes the 2 new species and *Uvulifer ambloplitis* (Hughes, 1927), as well as *Uvulifer elongatus* Dubois, 1988, *Uvulifer prosocotyle* (Lutz, 1928), and *Uvulifer weberi* Dubois, 1985, none of which have been part of prior molecular phylogenetic studies. Our data on *Uvulifer* revealed 0.1–2.2% interspecific divergence in *28S* sequences and 9.3–15.3% in *COI* sequences. Our *28S* phylogeny revealed at least 6 well-supported clades within the genus. In contrast, the branch topology in the *COI* phylogenetic tree was overall less supported, indicating that although *COI* sequences are a great tool for species differentiation, they should be used with caution for phylogenetic inference at higher taxonomic levels. Our *28S* phylogeny did not reveal any clear patterns of host association between *Uvulifer* and particular species of kingfishers; however, it identified 2 well-supported clades uniting *Uvulifer* species from distant geographical locations and more than 1 biogeographic realm, indicating at least 2 independent dispersal events in the evolutionary history of the New World *Uvulifer*. Our results clearly demonstrate that the diversity of *Uvulifer* in the New World has been underestimated.

The digenean genus *Uvulifer* Yamaguti, 1934 (Diplostomidae: Crassiphialinae), contains between 16 and 19 species worldwide, with the majority of the species parasitic in kingfishers (see Dubois, 1964; Yamaguti, 1971; Subair et al., 2013). The known life cycles for species of *Uvulifer* have a *Neascus*-type metacercaria that encysts on an aquatic vertebrate intermediate host, normally a fish (Hunter, 1933; Niewiadomska, 2002). Often the metacercariae become melanized by the fish host, which manifests as black spot disease (Niewiadomska, 2002; McAllister et al., 2013). Prior to this study, 6 valid species of *Uvulifer* were recognized from the Americas. Two of these species are distributed only in the Nearctic, 3 are distributed only in the Neotropics, and 1 species is distributed in both the Nearctic and Neotropics (Dubois, 1938, 1985, 1988; Muzzall et al., 2011; López-Jiménez et al., 2018). *Uvulifer ambloplitis* (Hughes, 1927) and *Uvulifer semicircumcisus* Dubois and Rausch, 1950, infect the belted kingfisher, *Megaceryle alcyon* (Linnaeus), in North America (Hunter, 1933; Dubois and Rausch, 1950). *Uvulifer prosocotyle* (Lutz, 1928) was reported from the ringed kingfisher, *Megaceryle torquata* Linnaeus, in Brazil and the Amazon kingfisher, *Chloroceryle amazona* (Latham), in Venezuela (Dubois, 1938; Caballero and Diaz-Ungria, 1958). *Uvulifer weberi* Dubois, 1985, is known from *C. amazona*, the green kingfisher, *Chloroceryle americana* (Gmelin), and the green-and-rufous kingfisher, *Chlor-*

Version of Record, first published online with fixed content and layout, in compliance with ICZN Arts. 8.1.3.2, 8.5, and 21.8.2 as amended, 2012. ZooBank Publication Record: urn:lsid:zoobank.org:pub:8CCC5507-3E1D-463B-AB9A-DC53DD1C9A0C.

ocerylе inda (Linnaeus), in Paraguay (Dubois, 1985, 1988). *Uvulifer elongatus* Dubois, 1988, was described from *M. torquata* in Paraguay (Dubois, 1988), and *Uvulifer spinatus* López-Jiménez, Pérez-Ponce de León, and García-Varela, 2018, was recently described from *C. americana* in Mexico and is also found in Guatemala, Honduras, and Nicaragua (López-Jiménez et al., 2018).

In the present study, we describe 2 previously unknown species of *Uvulifer* from *C. inda* in the Cordillera Azul National Park, Peruvian Amazon. We generated partial sequences of the nuclear large subunit ribosomal RNA gene (*28S*) and the mitochondrial cytochrome oxidase 1 gene (*COI*) from both new species and 5 additional species of *Uvulifer* collected from various kingfishers from South and North America and a fish from North America. Newly generated sequences were aligned and compared, and observed differences were used for augmenting morphological comparisons among species. Phylogenetic analyses were conducted independently for both gene fragments using new sequence data plus available congeneric sequence data from GenBank.

MATERIALS AND METHODS

Adult specimens belonging to the genus *Uvulifer* were obtained from *C. inda* collected in the Cordillera Azul National Park, Peru, *C. americana* and *M. torquata* from Pantanal, Fazenda Retiro Novo, Municipality of Poconé, Mato Grosso State, Brazil, *M. torquata* from the vicinities of Lábrea, state of Amazonas, Brazil, and *M. alcyon* from Minnesota. In addition, a metacercaria of *Uvulifer* sp. was collected from a yellow perch, *Perca flavescens* Mitchill, from Minnesota. Live digeneans removed from the hosts were briefly rinsed in saline, killed with hot water, and preserved in 80% ethanol. Specimens for light microscopy were stained with aqueous alum carmine or Mayer's hematoxylin following Lutz et al. (2017), dehydrated in an ethanol series of ascending concentration, cleared in clove oil, and mounted permanently in Damar gum. Specimens were identified and measured using an Olympus© BX53 microscope (Olympus America, Center Valley, Pennsylvania) equipped with a drawing tube and a digital imaging system operated through iSolution Lite software (Image & Microscope Technology Inc., Vancouver, British Columbia, Canada). All measurements given in the text are in micrometers unless otherwise stated. Type specimens of the new species and adult *Uvulifer* spp. are deposited in the collection of the Harold W. Manter Laboratory (HWML), University of Nebraska State Museum, Lincoln, Nebraska. We use the terms prosoma and opisthosoma instead of the often used anterior and posterior segments to reflect the fact that these parts of the body in diplostomoideans are not segments (e.g., unlike segments or proglottides in cestodes).

Genomic DNA was extracted from 1 whole individual of each of the new species using the methods described by Tkach and Pawlowski (1999). An approximate 1,300-bp-long fragment at the 5′ end of the *28S* rDNA gene (including variable domains D1–D3) was amplified from genomic DNA using the polymerase chain reaction (PCR) protocols in Tkach et al. (2003) and Tkach and Curran (2015), with the same primers used by Tkach and Curran (2015). A fragment of the mitochondrial cytochrome *c* oxidase subunit 1 (*COI*) gene was amplified using the previously published forward primer Cox1_Schist_5′ (5′–TCT TTR GAT CAT AAG CG–3′) and reverse primers acox650R (5′–CCA AAA AAC CAA AAC ATA TGC TG–3′) or JB5 (5′–AGC ACC TAA ACT TAA AAC ATA ATG AAA ATG–3′) (Lockyer et al., 2003; Derycke et al. 2005; Kudlai et al., 2015). In some cases, *COI* was amplified in 2 overlapping fragments using a combination of published primers and new internal primers designed for this study by TJA. The forward primer Cox1_Schist_5′ was used with the new reverse primer BS_CO1_IntR (5′–TAA TAC GAC TCA CTA TAA AAA AAA MAM AGA AGA RAA MAC MGT AGT AAT–3′); the new forward primer BS_CO1_IntF (5′–ATT AAC CCT CAC TAA ATG ATT TTT TTY TTT YTR ATG CC–3′) was used with the reverse primer acox650R. The underlined portions indicate a shortened T3 and T7 tail sequence.

PCR products were purified using the ExoSap PCR clean-up enzymatic kit from Affymetrix (Santa Clara, California) following the manufacturer's protocol. PCR products were cycle-sequenced directly using BrightDye® Terminator Cycle Sequencing Kit (MCLAB, San Francisco, California) chemistry, alcohol precipitated, and run on an ABI 3130 automated capillary sequencer (Life Technologies, Grand Island, New York).

PCR primers and the additional internal forward primer DPL600F (5′–CGG AGT GGT CAC CAC GAC CG–3′) and reverse primer DPL700R (5′–CAG CTG ATT ACA CCC AAA G–3′) were used for sequencing of *28S* PCR reactions (Achatz et al., 2019). The PCR primers were used for sequencing of *COI* PCR reactions. In addition, the shortened T3 tail (5′–ATT AAC CCT CAC TAA A–3′) and shortened T7 tail (5′–TAA TAC GAC TCA CTA TA–3′) primers from Van Steenkiste et al. (2015) were used for sequencing of the PCR reactions prepared with BS_COI_IntF and BS_COI_IntR primers. Contiguous sequences were assembled using Sequencher version 4.2 software (Gene-Codes Corp., Ann Arbor, Michigan). Newly generated sequences are deposited in GenBank (Table I).

Phylogenetic interrelationships among members of *Uvulifer* were analyzed using *28S* and *COI* datasets as separate alignments. Newly obtained and previously published sequences were aligned with Clustal W (Larkin et al., 2007) as implemented in BioEdit version 7.0.5.3 software (Hall, 1999); both alignments were trimmed to the length of the shortest respective sequence. *Ornithodiplostomum scardinii* (Shulman, 1952) was used as an outgroup in the *28S* analysis, and *O. scardinii* and *Posthodiplostomum centrarchi* Hoffman, 1958, were used in *CO1* analysis based on the topologies presented in the phylogenetic study by López-Jiménez et al. (2018).

The *28S* alignment included newly generated sequences of 7 species of *Uvulifer* and previously published sequences of 6 species-level lineages of *Uvulifer*, only 1 of them (*U. spinatus*) representing an identified species. The *COI* alignment included newly generated sequences of 7 species of *Uvulifer* and a single previously published compatible sequence of *Uvulifer* sp. Additional *COI* sequences of *Uvulifer* available in GenBank were non-compatible with our sequences or were much shorter in length.

Independent phylogenetic analyses (separate *28S* rRNA and *COI* gene alignments) were conducted using Bayesian Inference (BI) as implemented in MrBayes Ver. 3.2.6 software (Ronquist and Huelsenbeck, 2003). The general time-reversible model with estimates of invariant sites and gamma-distributed among-site variation (GTR + I + G) was identified as the best-fitting nucleotide substitution model for the 28S dataset using Mega7 (Kumar et al., 2016). The Hasegawa-Kishino-Yano and gamma-distributed among-site variation (HKY + G) model was identified

Table I. List of diplostomid species used in our phylogenetic analyses of *28S* rDNA and *COI* mtDNA including their host species, geographical origin of material, morphological voucher numbers, and GenBank accession numbers. CNHE: Colección Nacional de Helmintos, Instituto de Biología, Universidad Nacional Autónoma de México, Mexico City. Specimen 98.01_BLV is deposited in the collection of the Biodiversity Institute of Ontario.

Digenean taxa	Host species	Geographic origin	Museum no.	Accession no.		Reference
				28S	*COI*	
Ornithodiplostomum scardinii	*Scardinius erythrophthalmus*	Czech Republic	–	KX931427	KX931425	Stoyanov et al., 2017
Posthodiplostomum centrarchi	*Ardea herodias*	Canada	98.01_BLV	–	MH581291	Locke et al., 2018
Uvulifer ambloplitis	*Megaceryle alcyon*	U.S.A.	HWML-139982	MK874320	MK871329	Present study
Uvulifer batesi n. sp.	*Chloroceryle inda*	Peru	HWML-139983, HWML-139984	MK874321	MK871330	Present study
Uvulifer elongatus	*Megaceryle torquata*	Lábrea, Brazil	–	MK874322	MK871331	Present study
U. elongatus	*M. torquata*	Pantanal, Brazil	HWML-139985	MK874323	MK871332	Present study
Uvulifer pequenae n. sp.	*C. inda*	Peru	HWML-139986, HWML-139987	MK874324	MK871333	Present study
Uvulifer prosocotyle	*M. torquata*	Pantanal, Brazil	HWML-139988	MK874325	MK871334	Present study
Uvulifer spinatus	*Poecilia mexicana*	Mexico	CNHE: 10322–10324	MF568582	–	López-Jiménez et al., 2018
Uvulifer weberi	*Chloroceryle americana*	Pantanal, Brazil	HWML-139989	MK874326	MK871335	Present study
Uvulifer sp.	*Lepomis gibbosus*	Canada	–	–	MF124281	Blasco-Costa and Locke, 2017
Uvulifer sp.	*M. alcyon*	Mexico	–	MF398332	–	Hernández-Mena et al., 2017
Uvulifer sp.	*M. alcyon*	Mexico	–	MF568569	–	López-Jiménez et al., 2018
Uvulifer sp.	*Poecilia* sp.	Mexico	–	MF568674	–	López-Jiménez et al., 2018
Uvulifer sp.	*Amatitlania nigrofasciata*	Mexico	–	MF568575	–	López-Jiménez et al., 2018
Uvulifer sp.	*Tilapia sparrmanii*	South Africa	–	MK604825	–	Hoogendoorn et al., 2019
Uvulifer sp.	*Perca flavescens*	U.S.A.	–	MK874327	MK871336	Present study

as the best-fitting nucleotide substitution model for each of the partitioned nucleotide codon position. BI analyses were performed using MrBayes software as follows: Markov chain Monte Carlo (MCMC) chains were run for 3,000,000 generations with a sample frequency of 1,000, log-likelihood scores were plotted, and only the final 75% of trees were used to produce the consensus trees by setting the "burn-in" parameter at 750. This number of generations was considered sufficient because the SD dropped below 0.01. The trees were visualized in FigTree ver. 1.4 software (Rambaut, 2016) and annotated in Adobe Illustrator®.

DESCRIPTION

Uvulifer pequenae n. sp.

(Figs. 1, 2)

Description (based on 2 fully mature specimens): Body 1,403–1,432 long, comprising a prosoma and opisthosoma; prosoma pyriform, ventrally concave, 480–517 long, with maximum width in the posterior half (304–318); opisthosoma elongated, 922–932 long and claviform with maximum width near midpoint (202–236). Prosoma: opisthosoma length ratio 0.54–0.57. Tegumental spines covering prosoma but limited to anterior 25% of opisthosoma. Oral sucker nearly terminal, 68–77 × 88–99. Prepharynx absent or not apparent. Pharynx oval, 45–56 × 34–37. Esophagus slightly longer than pharynx. Cecal bifurcation in anterior third of prosoma. Ceca slender, blind, extending to near posterior end of opisthosoma. Ventral sucker delicate, much smaller than oral sucker, 39–40 × 45–48, located at 60–62% of the prosoma length from the anterior end. Tribocytic organ immediately posterior to ventral sucker (72% of the prosoma length from the anterior end); oval with ventral muscular portion having a longitudinal slit-like opening and basal glandular portion embedded in the prosoma, 133–136 × 99–114. Testes tandem, with smooth or slightly irregular margins, anterior testis 167–173 × 142–156, posterior testis 97–153 × 77–82. Seminal vesicle subglobular, ventral to posterior testis, connected to ejaculatory duct; proximal ejaculatory duct tubular and running antero-dorsally, then bending and running posteriorly; distal portion opening into a muscular ejaculatory pouch. Ejaculatory pouch 142–156 × 71–85, draining posteriorly through narrow short male duct posteriorly; duct uniting with female system. Ovary submedian, (slightly dextral), immediately pretesticular (32% of the opisthosoma length from the anterior end), subspherical, 79–85 × 82–91. Ootype surrounded by Mehlis' gland, submedian, (slightly dextral), intertesticular. Seminal receptacle subspherical, immediately dorsal to ootype, smaller than ovary. Uterus ventral in opisthosoma, extending from ovarian level to posterior margin of posterior testis, containing from 2 to 5 eggs (71–81 × 46–57); distal uterus uniting with male duct and forming hermaphroditic canal; hermaphroditic canal descending into genital cone. Genital cone 60–65 × 94–97, extends into a bulbous copulatory bursa; copulatory bursa with muscular ventral preputial fold. Ventrolateral preputial lobe 45–65 × 82–94. Vitelline follicles located in opisthosoma, ventral and lateral to gonads, absent in the anterior 13–16% of the opisthosoma and posterior 11–12% of opisthosoma. Vitelline reservoir intertesticular, sinistral to ootype. Excretory vesicle I-shaped, with main stem dorsal in opisthosoma; stem ascending into prosoma and surrounding tribocytic organ and giving rise to 6 longitudinal

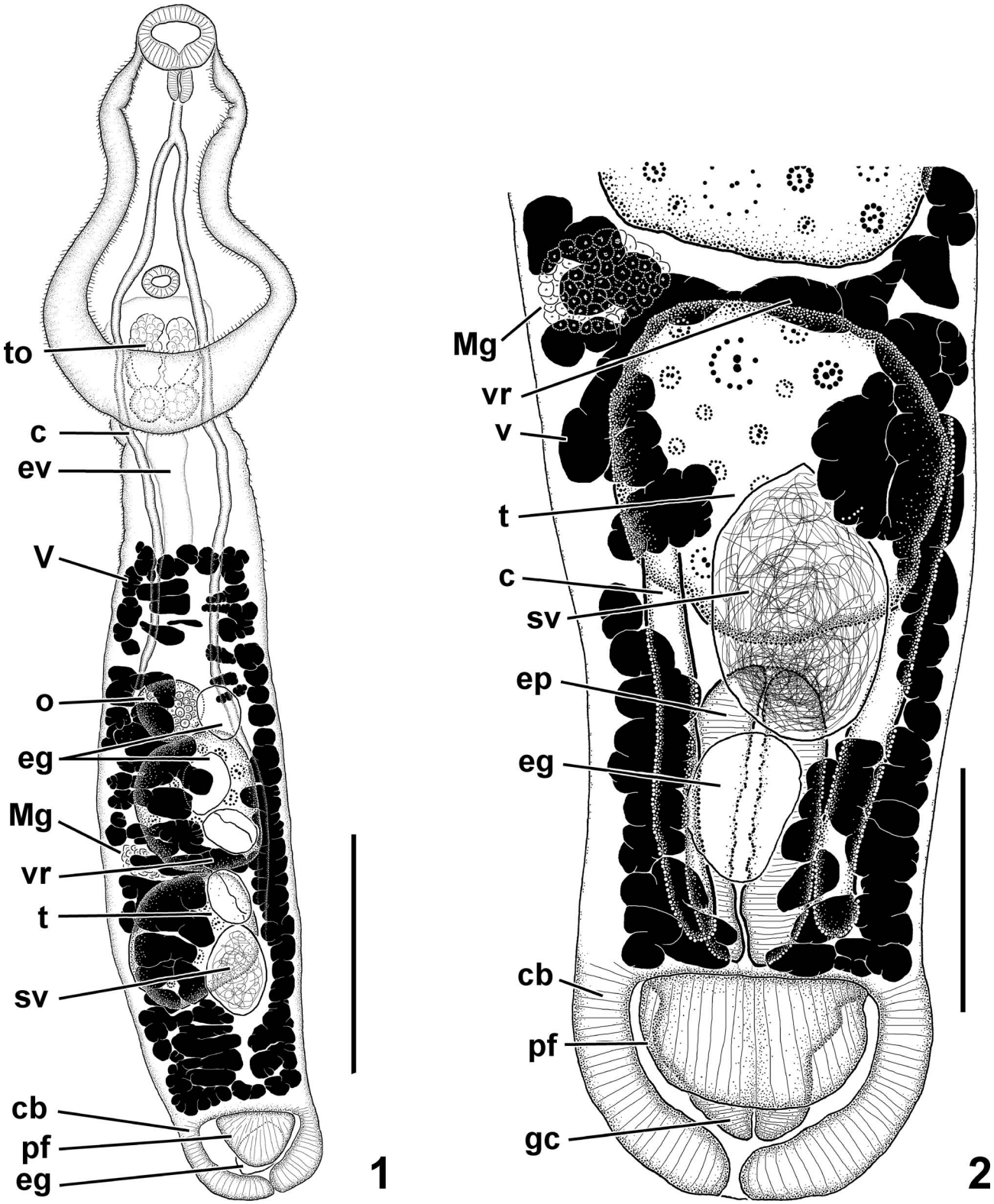

Figures 1, 2. *Uvulifer pequenae* n. sp. **(1)** Ventral view of whole mount. Scale bar = 300 μm. (**2**) Ventral view of posterior body end. Scale bar = 100 μm. Abbreviations: c, ceca; cb, copulatory bursa; eg, egg; ep, ejaculatory pouch; ev, excretory vesicle; gc, genital cone; Mg, Mehlis' gland; o, ovary; pf, preputial fold; sv, seminal vesicle; t, testis; to, tribocytic organ; v, vitelline follicle; vr, vitelline reservoir.

branches that extend toward oral sucker; branches interconnected by network of anastomosing channels throughout prosoma. Excretory pore not observed.

Taxonomic summary

Type host: Chlorocerye inda (Linnaeus) (Coraciiformes: Alcedinidae).

Site of infection: Small intestine.

Type locality: San Martín, Tocache Province, Cordillera Azul National Park, Río Pescadero, NE of Shapaja (8°10.694′S, 76°13.422′W), Peru, elev. 953 m above sea level.

Type specimens deposited: The type series consists of 2 fully mature specimens deposited in the Harold W. Manter Laboratory. Holotype: HWML 139986, labeled ex. *C. inda*, small intestine, Cordillera Azul National Park, Peru, 13 Nov 2013, coll. K. Patitucci; paratype: HWML 139987, label identical to the holotype. Symbiotype deposited in the Field Museum, Chicago (FMNH 3859910).

Representative DNA sequences: GenBank MK874324 (*28S*), MK871333 (*CO1*).

ZooBank registration: urn:lsid:zoobank.org:act:ED554410-BFDC-4FBD-AC4B-38A4BAF9213D

Etymology: The species is named after Tatiana Z. Pequeño Saco who provided invaluable assistance in organizing the field collecting in the Cordillera Azul.

Remarks

The new species clearly belongs to *Uvulifer* based on the combination of characteristic features that include the vitelline follicles confined to the opisthosoma, the presence of a muscular ejaculatory pouch, and a muscular copulatory bursa containing a retractile or protrusible genital cone partially surrounded by a ventrolateral preputial muscular fold (Niewiadomska, 2002).

We believe only mature specimens of *Uvulifer* should be used for reliable morphological identification. *Uvulifer pequenae* is distinguishable from *U. elongatus*, *U. semicircumcisus*, *U. spinatus*, and *U. weberi* by relatively shorter vitellarium. The vitellarium of all these 4 species occupies almost the whole length of the opisthosoma, whereas in *U. pequenae* it is absent in the first 13–16% of the opisthosoma. The new species also differs from these 4 species by a greater prosoma:opisthosoma length ratio (see below).

Uvulifer pequenae can be further distinguished from *U. elongatus* by a much shorter body length (1,403–1,432 in the new species vs. 2,200–3,300 in *U. elongatus*), a much smaller ventral sucker (39–40 × 45–48 in the new species vs. 85–100 × 100–120 in *U. elongatus*), and slightly smaller eggs (71–81 in the new species vs. 80–90 in *U. elongatus*). The most dramatic difference between *U. pequenae* and *U. elongatus* is seen in the prosoma:opisthosoma length ratio. It equals 0.54–0.57 in the new species vs. only 0.17–0.19 in our well-fixed specimens of *U. elongatus* and 0.21 based on our measurements of the original line drawing of the type-specimen. Furthermore, *28S* sequences are 0.9% different and *COI* sequences are 13.3% different between the 2 species.

Uvulifer pequenae can be further distinguished from *U. semicircumcisus* by somewhat smaller eggs (71–81 in the new species vs. 80–102 in *U. semicircumcisus*). The prosoma:opisthosoma length ratio in *U. pequenae* is also larger compared to *U. semicircumcisus* (0.54–0.57 in the new species vs. 0.28–0.41 in *U. semicircumcisus*). Additionally, *U. semicircumcisus* has been reported only from North America, whereas this new species is from the Peruvian Amazon.

Uvulifer pequenae can be further distinguished from *U. spinatus* by a larger ventral sucker (39–40 × 45–48 in the new species vs. 21–28 × 28–35 in *U. spinatus*). The prosoma:opisthosoma length ratio in *U. pequenae* is also larger compared to *U. spinatus* (0.54–0.57 in the new species vs. 0.28–0.41 in *U. spinatus*). Our sequence of *U. pequenae 28S* was similar to *U. spinatus*; the 2 species differ by 0.4%, which is similar or greater than the differences recorded between other congeneric species within the Diplostomoidea Poirier, 1886 (Locke et al., 2018; Achatz et al., 2019). For example, *28S* sequences of 3 species of *Parastrigea* Szidat, 1928 published by Hernández-Mena et al. (2017) differ by only 0.09–0.71% (1 to 8 bases different out of 1,132). The previously published *COI* sequences of *U. spinatus* were not homologous with the sequence obtained in our study.

Uvulifer pequenae can be further distinguished from *U. weberi* by a larger oral sucker (68–77 × 88–99 in the new species vs. 45–57 × 48–57 in *U. weberi*) and larger tribocytic organ (133–136 × 99–114 in the new species vs. 60–95 × 60–80 in *U. weberi*). The prosoma:opisthosoma length ratio in *U. pequenae* is larger compared to *U. weberi* (0.54–0.57 in the new species vs. 0.41–0.44 in *U. weberi* based on our specimens, and 0.35 based on the original line drawing of the type-specimen). The *28S* sequence of *U. weberi* differs by 1.3% from that of *U. pequenae*, while *COI* sequences differ by 12.9%.

Uvulifer pequenae can be distinguished from *U. ambloplitis* as originally described by Hunter (1933) by having smaller eggs (71–81 long in the new species vs. 90–99 long in *U. ambloplitis*). The vitelline follicles do not reach the anterior margin of testes in *U. ambloplitis*, but extend anteriorly well beyond this level in the new species. Our sequences of *U. ambloplitis* and *U. pequenae* differ from each other by 1.4% in *28S* and 12.9% in *COI*. Additionally, adult *U. ambloplitis* have not been reported outside the Nearctic.

Uvulifer pequenae is morphologically closest to *U. prosocotyle*, especially in the prosoma:opisthosoma length ratio (0.54–0.57 in the new species vs. 0.46–0.77 in our specimens of *U. prosocotyle* and 0.75 based on the original line drawing of the type-specimen). The 2 species differ in the egg size (71–81 long in the new species vs. 83–90 long in *U. prosocotyle*), and the relative extent of vitelline fields. The vitellarium-free zone occupies the first 13–16% of the opisthosoma in the new species compared to approximately 22–33% in our specimens of *U. prosocotyle*. The vitellarium of *U. pequenae* extends to approximately halfway between the anterior margin of the ovary and the anterior margin of the opisthosoma. In contrast, the vitellarium of *U. prosocotyle* extends to approximately the anterior margin of the ovary. *Uvulifer prosocotyle* also has a very distinctive 'neck' region that is much narrower than the rest of the opisthosoma, whereas *U. pequenae* does not have this narrow part of the opisthosoma. Specimens of both *U. pequenae* and *U. prosocotyle* used in our study were heat-killed and fixed in the same manner. While the morphology of both species is very similar, the sequence divergence is very substantial at 1.4% in the *28S* sequence and 12.9% in *COI*. Complete comparison of metric characters for *U. pequenae* and *U. prosocotyle* is provided in Table II.

Table II. Metric characters of new *Uvulifer* spp. from Peru and the most morphologically similar congeners from the New World. Measurements of *Uvulifer spinatus* taken from López-Jiménez et al. (2018). Range values are followed by mean after semicolon.

Character	Species			
	Uvulifer pequenae n. sp. (n = 2)	*Uvulifer batesi* n. sp. (n = 2)	*Uvulifer prosocotyle* (n = 4)	*Uvulifer spinatus* (n = 13)
Geographic origin of material	Peru	Peru	Brazil	Mexico
Overall body length	1,403–1,432; 1,418	1,291–1,319; 1,305	1,060–1,439; 1,285	1,161–1,782; 1,499
Prosoma length	480–517; 499	307–335; 321	436–496; 460	276–439
Prosoma width	304–318; 311	251–285; 268	221–257; 235	204–227
Opisthosoma length	922–932; 927	1,032–1,034; 1,033	644–983; 846	800–1,327
Opisthosoma width	202–236; 219	170–195; 183	168–203; 183	110–195
Oral sucker length	68–77; 73	43–44; 44	55–73; 63	57–71; 61
Oral sucker width	88–99; 94	48–51; 50	106–113; 109	53–74; 62
Pharynx length	45–56; 51	23–25; 24	48–58; 54	34–46; 37
Pharynx width	34–37; 36	20	38–51; 43	29–35; 32
Ventral sucker length	39–40; 40	25–26; 26	35–38; 37	21–28; 24
Ventral sucker width	45–48; 47	29–31; 30	42–47; 45	28–35; 31
Tribocytic organ length	133–136; 135	105	73–106; 88	88–121; 97
Tribocytic organ width	99–114; 107	85	68–80; 75	97–125; 108
Ovary length	79–85; 82	Obscured by uterus	56–70; 62	49–72; 59
Ovary width	82–91; 87	Obscured by uterus	60–74; 65	56–64; 60
Anterior testis length	167–173; 170	91–94; 93	118–150; 136	80–144; 113
Anterior testis width	142–156; 149	85–97; 91	122–146; 131	91–125; 108
Posterior testis length	97–153; 125	97–107; 102	119–171; 138	78–139; 104
Posterior testis width	77–82; 80	94–97; 96	116–137; 124	89–124; 107
Genital cone length	60–65; 63	74–80; 77	61–94; 78	71–117; 89
Genital cone width	94–97; 96	80–86; 83	55–88; 67	–
Ejaculatory pouch length	142–156; 149	111	Not well observed	110–217; 172
Ejaculatory pouch width	71–85; 78	60–63; 62	Not well observed	64–109; 80
Egg number	2–5; 4	4–6; 5	0–3	–
Egg length	71–81; 76	76–87; 82	83–90; 88	65–81; 73
Egg width	46–57; 53	41–52; 47	43–44; 44	42–48; 44
Ventrolateral preputial lobe length	45–65; 55	68–99; 84	42–59; 50	–
Ventrolateral preputial lobe width	82–94; 88	130–142; 136	76–103; 89	–
Prosoma:opisthosoma length ratio	0.54–0.57; 0.56	0.31–0.33; 0.32	0.46–0.77; 0.56	0.28–0.41*
Oral sucker:ventral sucker width ratio	1.76–2.31; 2.04	1.39–1.52; 1.46	2.28–2.52; 2.44	1.67–2.33; 1.99
Anterior vitellarium-free zone: opisthosoma length	0.13–0.16; 0.15	0.25–0.28; 0.27	0.22–0.33; 0.25	–
Posterior vitellarium-free zone: opisthosoma length	0.11–0.12; 0.12	0.15–0.16; 0.16	0.12–0.14; 0.14	–
Anterior margin of ventral sucker positioned at	60–62% of prosoma length; 61%	37–39% of prosoma length; 38%	57–62% of prosoma length; 59%	–
Anterior margin of holdfast positioned at	72% of prosoma length	46–47% of prosoma length; 46.5%	66–72% of prosoma length; 69%	–
Anterior margin of ovary positioned at	32% of opisthosoma length	50–53% of opisthosoma length; 51.5%	27–45% of opisthosoma length; 36%	–

* Originally given as opisthosoma: prosoma length ratio by López-Jiménez et al. (2018).

***Uvulifer batesi* n. sp.**
(Figs. 3, 4)

Description (based on 2 fully mature specimens): Body 1,291–1,319 long, comprising prosoma and opisthosoma; prosoma oval, ventrally concave, 307–335 long, with maximum width at midway (251–285); opisthosoma elongated, 1,032–1,034, gradually widening toward bell-shaped posterior end (170–195). Prosoma:opisthosoma length ratio 0.31–0.33. Prosoma devoid of tegumental spines, opisthosoma (excluding bell-shaped posterior end) covered by tegumental spines. Oral sucker nearly terminal, 43–44 × 48–51. Prepharynx absent. Pharynx oval, overlapping with oral sucker, 23–25 × 20. Esophagus about equal in length with pharynx. Cecal bifurcation in anterior third of prosoma. Ceca slender, blind, extending to near posterior end of opisthosoma. Ventral sucker delicate, much smaller than oral sucker, 25–26 × 29–31, located 37–39% of the prosoma length from the anterior end. Tribocytic organ 105 × 85, located immediately posterior to ventral sucker (46–47% of the prosoma length from the anterior end), oval with ventral muscular portion having a deep, longitudinal slit-like opening and basal glandular portion embedded in the prosoma. Testes tandem, with smooth margins, anterior testis 91–94 × 85–

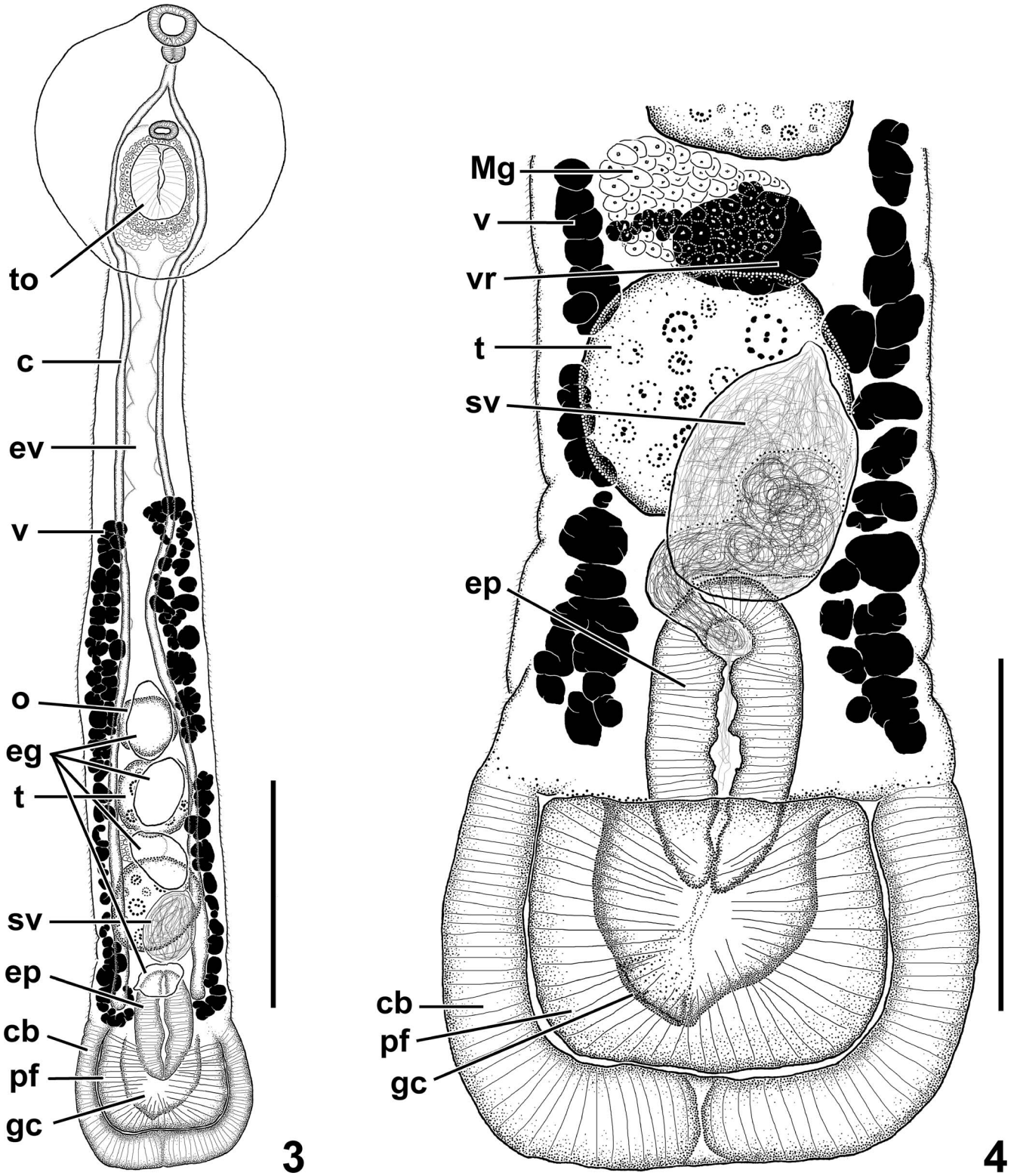

Figures 3, 4. *Uvulifer batesi* n. sp. **(3)** Ventral view of holotype. Scale bar 250 μm. **(4)** Ventral view of posterior body end of holotype with uterus omitted. Scale bar = 150 μm. Abbreviations: c, ceca; cb, copulatory bursa; eg, egg; ep, ejaculatory pouch; ev, excretory vesicle; gc, genital cone; Mg, Mehlis' gland; o, ovary; pf, preputial fold; sv, seminal vesicle; t, testis; to, tribocytic organ; v, vitelline follicle; vr, vitelline reservoir.

97, posterior testis 97–107 × 94–97. Seminal vesicle subglobular, ventral to posterior testis, connected to ejaculatory duct; proximal ejaculatory duct funnel-like with proximal end wide and distal end narrowing and running antero-dorsally, then bending and running posteriorly; distal portion opening into a muscular ejaculatory pouch; ejaculatory pouch 111 × 60–63, draining posteriorly through narrow short male duct. Ovary appearing subspherical with smooth margin (but largely obscured by uterus in both specimens), immediately pretesticular (50–53% of the opisthosoma length from the anterior end). Ootype surrounded by Mehlis' gland, submedian (slightly dextral), intertesticular. Seminal receptacle not observed. Uterus ventral in opisthosoma, extending from a level slightly pre-ovarian to posterior margin of posterior testis, containing 4–6 eggs (76–87 × 41–52); distal uterus uniting with male duct and forming hermaphroditic canal; hermaphroditic canal descending into genital cone. Genital cone 74–80 × 80–86, extending into a highly bulbous copulatory bursa; copulatory bursa with prominent muscular ventrolateral preputial fold. Ventrolateral preputial fold 68–99 × 130–142. Vitelline follicles in opisthosoma, ventral, absent in the anterior 25–28% of the opisthosoma and posterior 15–16% of opisthosoma. Vitelline reservoir intertesticular, sinistral to ootype. Excretory vesicle I-shaped, with main stem dorsal in opisthosoma; main stem appearing wavy, ascending into prosoma and surrounding tribocytic organ and giving rise to 6 secondary longitudinal branches that extend toward oral sucker; branches surrounding suckers and interconnected by network of anastomosing channels throughout prosoma. Excretory pore not observed.

Taxonomic summary

Type host: Chloroceryle inda (Linnaeus) (Coraciiformes: Alcedinidae).

Site of infection: Small intestine.

Type locality: San Martín, Tocache Province, Cordillera Azul National Park, Río Pescadero, NE of Shapaja (8°10.694′S, 76°13.422′W), Peru, elev. 953 m above sea level.

Type specimens deposited: The type series consists of 2 fully mature specimens deposited in the Harold W. Manter Laboratory. Holotype: HWML 139983, labeled ex. *C. inda*, small intestine, Cordillera Azul National Park, Peru, 13 Nov 2013, coll. K. Patitucci; paratype: HWML-139984, labeled identical to the holotype. Symbiotype deposited in the Field Museum, Chicago (FMNH 3859910).

Representative DNA sequences: GenBank MK874321 (*28S*), MK871330 (*CO1*).

ZooBank registration: urn:lsid:zoobank.org:act:F23BE7CF-0942-404F-AD5F-E2E2D373A4AE

Etymology: The new species is named after Dr. John Bates in recognition of his contributions to the knowledge of South American birds and as the leader of the field crew that collected the new species.

Remarks

The new species clearly belongs to *Uvulifer* based on the combination of characteristic features such as the presence of a muscular ejaculatory pouch and a muscular copulatory bursa containing a retractile or protrusible genital cone partially surrounded by a ventrolateral preputial muscular fold.

Uvulifer batesi is easily distinguished from the New World congeners by the wide, bell-shaped copulatory bursa region at the posterior body end. This is the widest portion of the opisthosoma in *U. batesi*, whereas the widest part of the opisthosoma in other New World congeners is at the testicular level.

Uvulifer batesi can also be distinguished from *U. elongatus*, *U. semicircumcisus*, *U. spinatus*, and *U. weberi* by relatively shorter vitellarium. The vitellarium in all these 4 species occupies almost the whole length of the opisthosoma, whereas in *U. batesi* it is absent in the first 25–28% of the opisthosoma.

Uvulifer batesi can be further differentiated from *U. elongatus* by shorter body length (1,291–1,319 in the new species vs. 2,200–3,300 in *U. elongatus*), a much smaller ventral sucker (25–26 × 29–31 in the new species vs. 85–100 × 100–120 in *U. elongatus*), and pharynx (23–25 × 20 in the new species vs. 45–55 × 30–37 in *U. elongatus*). In addition, *U. batesi* and *U. elongatus* differ by 0.9% in *28S* sequences and 12.9% in *COI* sequences.

Uvulifer batesi can be further distinguished from *U. semicircumcisus* by a thinner opisthosoma (170–195 in the new species vs. 270–400 in *U. semicircumcisus*) and smaller ventral sucker (25–26 × 29–31 in the new species vs. 40–49 in diameter in *U. semicircumcisus*). Additionally, *U. semicircumcisus* has been reported only in North America, whereas *U. batesi* was found in the Peruvian Amazon.

Uvulifer batesi can be further differentiated from the morphologically similar *U. spinatus* by the distribution of tegumental spines. In *U. batesi* the tegumental spines cover the majority of the opisthosoma, whereas in *U. spinatus* they extend only from the anterior margin of the opisthosoma to the anterior testis. Additionally, the 2 species can be differentiated by the more posteriorly positioned gonads in *U. batesi*, a smaller pharynx (23–25 × 20 in this new species vs. 34–46 × 29–35 in *U. spinatus*), and a smaller oral sucker:ventral sucker width ratio (1.39–1.52 in this new species vs. 1.67–2.33 in *U. spinatus*). The *28S* sequence of *U. batesi* was similar to that of *U. spinatus*; the 2 species differ by only 0.3%. The available *COI* sequences of *U. spinatus* were not homologous with our sequences. Complete comparison of metric characters for *U. pequenae* and *U. prosocotyle* is provided in Table II.

Uvulifer batesi can be further distinguished from *U. weberi* by the somewhat, relatively more posterior gonads in *U. batesi*. In addition, both *28S* (1.3%) and *COI* (13.7%) sequences are quite different between the 2 species.

Uvulifer batesi can be further distinguished from *U. ambloplitis*, as originally described by Hunter (1933), by having a smaller oral sucker (43–44 × 48–51 in the new species vs. 94–120 diameter in *U. ambloplitis*), smaller pharynx (23–25 × 20 in our new species vs. 52–63 × 40–45 in *U. ambloplitis*), smaller ventral sucker (25–26 × 29–31 in our new species vs. 44–52 × 45–56 in *U ambloplitis*), smaller eggs (76–87 in our new species vs. 90–99 in *U. ambloplitis*), and relatively longer fields of vitelline follicles that do not reach the anterior margin of testes in *U. ambloplitis* but extend well beyond this level anteriorly in *U. batesi*. Our sequences of *U. ambloplitis* and *U. batesi* are 1.4% different in *28S* and 15.1% different in *COI*. As stated above, adult specimens of *U. ambloplitis* have been reported only in the Nearctic, whereas *U. batesi* is from the Peruvian Amazon.

Uvulifer batesi can be further differentiated from *U. prosocotyle* by the lower prosoma:opisthosoma length ratio (0.31–0.33 in the new species vs. 0.46–0.77 in our specimens of *U. prosocotyle* and

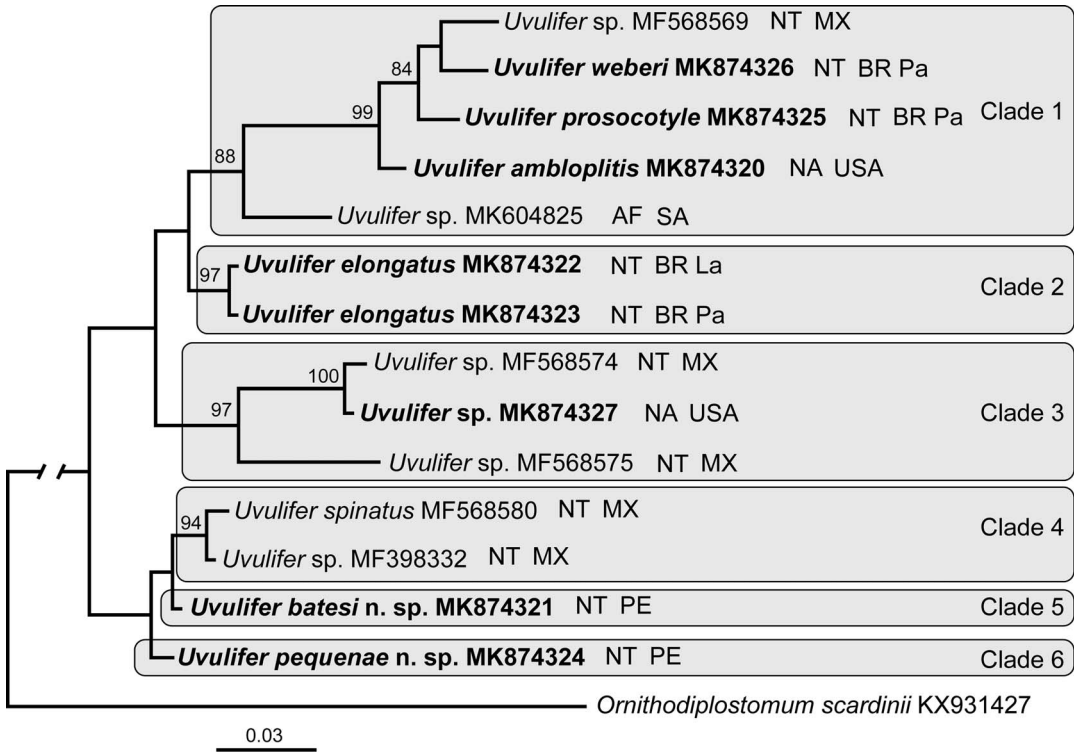

Figure 5. Phylogenetic interrelationships among 14 *Uvulifer* taxa based on Bayesian Inference (BI) analysis of partial *28S* rRNA gene sequences. Bayesian Inference posterior probability values lower than 70% (BI) are not shown. New sequences obtained in this study are in bold. Branch length scale bar indicates number of substitutions per site. GenBank accession numbers and the biogeographical realm, and geographic origin are provided after the names of species. Abbreviations for biogeographical realms: AF = Afrotropical realm, NA = Nearctic realm, NT = Neotropical realm. Abbreviations for geographic origin: BR La = Lábrea site in Brazil, BR Pa = Pantanal site in Brazil, MX = Mexico, PE = Peru, SA = South Africa, USA = United States of America.

0.75 based off the original line drawing of the type-specimen). In addition, *U. prosocotyle* also has a very distinctive 'neck' region that is much narrower than the rest of the opisthosoma, while *U. batesi* does not have this narrowed part of the opisthosoma. In addition, the 2 species differ by 1.4% in *28S* sequences and by 13.1% in *COI* sequences.

Uvulifer batesi can be further distinguished from *U. pequenae* by the lower prosoma: opisthosoma length ratio (0.31–0.33 in the new species vs. 0.54–0.57 in *U. pequenae*) and the distribution of tegumental spines. The tegumental spines of *U. batesi* cover most of the opisthosoma but are completely absent on the prosoma. In contrast, the anterior 25% of the opisthosoma and entire prosoma have tegumental spines in *U. pequenae*. The *28S* sequences were very close with only 0.2% difference; however, the *COI* sequences showed a much greater difference of 10%.

Molecular phylogenies

Upon trimming to the length of the shortest sequence the *28S* alignment was 1,133 bp long. The phylogenetic tree resulting from the BI analysis contained 6 *Uvulifer* clades (Fig. 5). The clade 1 (88%) included recently published *Uvulifer* sp. (MK604825) from South Africa and a well-supported clade (99%) of *U. ambloplitis* + *U. prosocotyle* + *U. weberi* + *Uvulifer* sp. (GenBank accession MF568569). Notably, this clade included species from the Afrotropics, Nearctic, and Neotropics. The clade 2 (97%) included both of our isolates of *U. elongatus* collected from Amazonas (Lábrea) and Mato Grosso (Pantanal) states in Brazil. The clade 3 (97% support) was composed of *Uvulifer* sp. (MF568575) + a well-supported clade (100%) of *Uvulifer* sp. (MF568574) + *Uvulifer* sp. (MK874327). This clade was composed of only metacercariae from species from the Nearctic and Neotropics. The clade 4 (94% support) included *U. spinatus* + *Uvulifer* sp. (GenBank MF398332). Clades 5 and 6 included a single species each, *U. pequenae* and *U. batesi*.

Upon trimming to the length of the shortest sequence the *COI* alignment was 451 bp long. While the branch topology of the *Uvulifer* tree was reasonably resolved, the support of the majority of nodes was rather weak (Fig. 6). The 2 new species from Peru appeared on the tree as sister taxa to the rest of the species in the genus. Despite some difference in the composition of the included species the *28S* and *CO1* phylogenies had an overall very similar branch topology.

Genetic variation

The interspecific divergence in *28S* sequences of *Uvulifer* spp. was generally low (0.1–2.2% or 1–25 bases out of 1,132). In contrast, *COI* sequences had much greater interspecific variation (9.3–15.3% or 42–69 bases out of 451). Although the 2 new *Uvulifer* species from the Peruvian Amazon were very similar in *28S* sequences (0.2% or 2 bases out of 1,132), they were 10% different (45 bases out of 451 bases) in *COI*. *Uvulifer pequenae* and its morphologically closest congener *U. prosocotyle* differ by 1.4% (16 bases out of 1,132 bases) in *28S* sequences and 12.9% (58 bases out of 451 bases) in *COI*. *Uvulifer batesi* and its

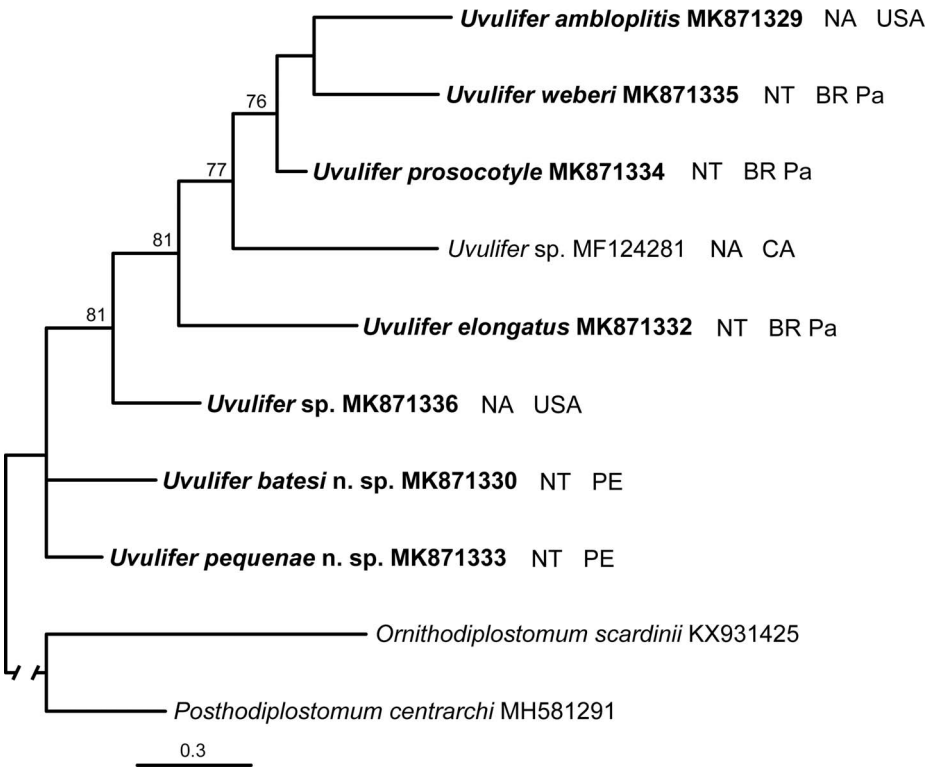

Figure 6. Phylogenetic interrelationships among 8 *Uvulifer* taxa based on Bayesian Inference (BI) analysis of partial *COI* mtDNA sequences. Bayesian Inference posterior probability values lower than 70% (BI) are not shown. New sequences obtained in this study are in bold. Branch length scale bar indicates number of substitutions per site. GenBank accession numbers, the biogeographical realm, and the geographic origin are provided after the names of species. Abbreviations for biogeographical realms: NA = Nearctic realm, NT = Neotropical realm. Abbreviations for geographic origin: BR Pa = Pantanal site in Brazil, CA = Canada, PE = Peru, USA = United States of America.

morphologically closest congener *U. spinatus* differ by 0.3% (3 bases out of 1,132 bases) in *28S* sequences (compatible *COI* sequences of *U. spinatus* are not available). Pairwise nucleotide comparisons among all *Uvulifer* spp. are provided in Tables III and IV. It is noteworthy that our isolate of *U. elongatus* from Pantanal, Brazil, had a single mixed base (a double peak) in its *28S* sequence, whereas our isolate of *U. elongatus* from Lábrea, Brazil, did not have any mixed bases in *28S*. There was only 0.5% difference (2 out of 426 bases) in their *COI* sequences.

DISCUSSION

The 2 new species of *Uvulifer* described herein represent the first species of *Uvulifer* described from Peru, and the seventh and eighth species of *Uvulifer* species in the New World. Our study is the first to provide DNA sequence data from *U. ambloplitis*, *U. elongatus*, *U. prosocotyle*, and *U. weberi*. Although a number of studies have involved *Uvulifer* (e.g., Boyd and Fry, 1971; Muzzall et al., 2011; Flores-Lopes, 2014), our study is only the fourth molecular phylogenetic study to produce DNA sequence data sourced from adult *Uvulifer* spp. (Hernández-Mena et al., 2017; López-Jiménez et al. 2018; Hoogendoorn et al., 2019) and only the second study to produce DNA sequence data from named adult material (López-Jiménez et al., 2018).

The interspecific genetic variation among partial *28S* sequences was lower than demonstrated by López-Jiménez et al. (2018) for *U. spinatus* and other unnamed lineages of *Uvulifer*. Our *28S* sequences of *Uvulifer* from South and North America demonstrated 0.2–1.6% interspecific divergence levels (Table III), which is lower than the range of 1.3–1.6% for interspecific differences reported by López-Jiménez et al. (2018). Interspecific divergence in our partial *COI* sequences showed levels of differences similar to those reported by López-Jiménez et al. (2018). Newly generated *COI* sequences showed 9.3–15.1% difference among species (Table IV), whereas López-Jiménez et al. (2018) reported 9.3–12.5% differences. The 2 genetically closest named species of *Uvulifer* in our dataset (*U. batesi* and *U. pequenae*) had only a 2 nucleotide difference in *28S* while demonstrating a much greater 10% difference in *COI* sequences. This suggests that as few as a 2 bases difference (assuming high sequence quality) in *28S* may be sufficient to differentiate between species in this genus, although it cannot be excluded that some species may have identical 28S sequences.

Our newly generated *COI* sequences cover the same region of *COI* as the vast majority of published *COI* sequences of diplostomoideans (e.g., sequences originating from Blasco-Costa and Locke, 2017; Hernández-Mena et al., 2017; Hoogendoorn et al., 2019). López-Jiménez et al. (2018) opted to amplify and sequence a different region of *COI* for their *Uvulifer* spp. We attempted amplification of the region sequenced by López-Jiménez et al. (2018) from our 2 new species. The PCRs were unsuccessful, although we did not experience problems amplifying and sequencing the *28S* fragment and the standard "barcoding" region of the *COI* gene. Only 2 of the newly generated *COI* sequences (from metacercaria MK871336 and *U. prosocotyle*

Table III. Pairwise comparisons of partial sequences of the *28S* rRNA gene between *Uvulifer* species included in this study. Percentage differences are given above diagonal and the number of variable nucleotide positions is given below the diagonal. The *28S* results are based on a 1,132-bp-long alignment.

	1. MK874320	2. MK874321	3. MK874323	4. MK874324	5. MK874325	6. MK874326	7. MF568582	8. MK874327	9. MF398332	10. MF568569	11. MF568674	12. MF568575	13. MK604825
1. *Uvulifer ambloplitis* MK874320	—	1.4%	1.2%	1.4%	0.5%	0.5%	1.5%	1.6%	1.4%	0.7%	1.7%	2%	1.2%
2. *Uvulifer batesi* n. sp. MK874321	16	—	0.9%	0.2%	1.4%	1.3%	0.3%	1.4%	0.2%	1.5%	1.3%	1.7%	1.2%
3. *Uvulifer elongatus* MK874323	13	10	—	0.9%	1.5%	1.4%	1.2%	1.2%	1.1%	1.6%	1.3%	1.5%	0.8%
4. *Uvulifer pequenae* n. sp. MK874324	16	2	10	—	1.4%	1.3%	0.4%	1.4%	0.4%	1.5%	1.3%	1.7%	1.2%
5. *Uvulifer prosocotyle* MK874325	6	16	17	16	—	0.5%	1.5%	1.6%	1.4%	0.5%	1.7%	2%	1.2%
6. *Uvulifer weberi* MK874326	6	15	16	15	6	—	1.6%	1.7%	1.5%	0.5%	1.8%	2%	1.6%
7. *Uvulifer spinatus* MF568582	17	3	13	5	17	18	—	1.7%	0.1%	1.6%	1.6%	2%	1.3%
8. *Uvulifer* sp. MK874327	18	16	14	16	18	19	19	—	1.6%	1.7%	0.1%	1.3%	1.4%
9. *Uvulifer* sp. MF398332	16	2	12	4	16	17	1	18	—	1.5%	1.5%	1.9%	1.2%
10. *Uvulifer* sp. MF568569	8	17	18	17	6	6	18	19	17	—	1.8%	2.2%	1.6%
11. *Uvulifer* sp. MF568674	19	15	15	15	19	20	18	1	17	20	—	1.4%	1.5%
12. *Uvulifer* sp. MF568575	22	19	17	19	22	23	22	15	21	25	16	—	1.6%
13. *Uvulifer* sp. MK604825	14	14	9	14	14	18	15	16	14	18	17	18	—

Table IV. Pairwise comparisons of partial sequences of the *COI* mtDNA gene between *Uvulifer* species included in this study. Percentage differences are given above diagonal and the number of variable nucleotide positions is given below the diagonal. Results are based on a 451-bp-long alignment.

	1. MK871329	2. MK871330	3. MK871332	4. MK871333	5. MK871334	6. MK871335	7. MK871336	8. MF124281
1. *Uvulifer ambloplitis* MK871329	—	15.1%	14.6%	12.9%	10.4%	11.5%	13.5%	13.7%
2. *Uvulifer batesi* n. sp. MK871330	68	—	12.9%	10%	13.1%	13.7%	11.3%	15.3%
3. *Uvulifer elongatus* MK871332	66	58	—	13.3%	11.3%	13.5%	14.2%	14.4%
4. *Uvulifer pequenae* n. sp. MK871333	58	45	60	—	12.9%	12.9%	10.4%	14.2%
5. *Uvulifer prosocotyle* MK871334	47	59	51	58	—	9.3%	10.4%	11.3%
6. *Uvulifer weberi* MK871335	52	62	61	58	42	—	13.3%	13.3%
7. *Uvulifer* sp. MK871336	61	51	64	47	47	60	—	12%
8. *Uvulifer* sp. MF124281	62	69	65	64	51	60	54	—

MK871334) overlapped with the region of the *COI* gene sequenced by López-Jiménez et al. (2018). Their sequence MF568574 and our metacercaria from Minnesota differ in *28S* only by a single nucleotide; however, in *COI* they differ by 4.9% (14 bases out of 283). This level of divergence is much lower than differences seen between other named *Uvulifer* species in the same region of *COI* (usually ~10% difference or more). It should be noted that according to López-Jiménez et al. (2018) the *COI* intraspecific variation in their material did not exceed 1.8%. Sequencing and morphological examination of a greater diversity of adult specimens from broader geographic area is necessary to determine if the metacercaria from our material is an independent species or represents a genetically divergent population of a known species.

Six species of kingfishers occur in the Americas. *Megaceryle alcyon* inhabits widespread areas of North America north of Mexico and may also winter in Central and South America. *Megaceryle torquata* inhabits ranges from the Rio Grande valley of North America south throughout Central America and South America. *Chloroceryle americana* is distributed throughout the southwestern United States south to central Argentina. *Chloroceryle amazona* ranges from Central America south to northern Argentina; the American pygmy kingfisher, *Chloroceryle aenea* (Pallas), ranges from southern Mexico south throughout central South America. The range of *Chloroceryle inda* extends from Nicaragua to Paraguay (Remsen, 1991). Our phylogenetic analyses included *Uvulifer* spp. from 4 New World kingfisher species: *M. alcyon, M. torquata, C. americana*, and *C. inda*. In the phylogeny resulting from our analysis of *28S* (Fig. 5), neither of the well-supported clades that included more than 1 species of *Uvulifer* was limited to a single kingfisher species. In part, this may be the result of the strong overlap of distributions of the South American kingfisher species. It is known that a species of kingfisher can be host to multiple species of *Uvulifer*; for instance, *U. pequenae* and *U. batesi* both parasitize *C. inda*, and at least 3 species of *Uvulifer* parasitize *M. alcyon* (Hernández-Mena et al., 2017; López-Jiménez et al., 2018; present data). However, the potential for a single *Uvulifer* species to infect multiple species of kingfisher has not been previously tested using molecular tools.

The phylogenetic tree based on the *28S* alignment (Fig. 5) revealed 2 strongly supported clades of *Uvulifer* containing specimens from distant geographical locations. Clade 1 included *Uvulifer* sp. from the Afrotropical realm, *U. ambloplitis* from the Nearctic, and *Uvulifer* sp., *U. weberi*, and *U. prosocotyle* from the Neotropics. The clade 3 included 2 unidentified species-level lineages distributed in Mexico and Central America (López-Jiménez et al., 2018) and a form from the northern United States. This likely indicates at least 2 independent dispersal events in the evolutionary history of the New World *Uvulifer*. The interrelationships and phylogeographic history of *Uvulifer* will likely be better resolved once DNA sequence data are available from a greater diversity of *Uvulifer* species including those from the Eastern Hemisphere.

The branch topology in the *COI* phylogenetic tree was not fully resolved and had overall lowed support values likely due to the mutation saturation effect. Somewhat higher branch support values in the *CO1* tree within *Uvulifer* reported by López-Jiménez et al. (2018) are likely explained by the fact that these authors sequenced a different, somewhat shorter and less variable region of *CO1* gene. Our results indicate that while *COI* sequences are a great tool for species differentiation, they should be used with caution for phylogenetic inference at higher taxonomic levels.

The result of our *COI* phylogeny (Fig. 6) confirmed the low utility of *COI* sequence data for phylogenetic inference in this digenean group that was suggested in the recent major publications on this group and digeneans overall (Locke et al., 2018; Pérez-Ponce de León and Hernández-Mena, 2019). Regardless, utilization of ribosomal as well as mitochondrial sequence data as tools for assisting with differentiating among species greatly enhances the power of taxonomic investigations within the Diplostomidae.

Our specimens of *U. ambloplitis* closely conform morphologically to the form originally described as *Uvulifer claviformis* Dubois & Rausch, 1948. Boyd and Fry (1971) later noted that Dubois viewed *U. claviformis* as a synonym of *U. ambloplitis* based on materials from Boyd and Fry (1971) and other materials in a personal communication. We believe the differences between the 2 forms can be possibly explained by the varying levels of

contraction after fixation and/or levels of maturity as noted by Boyd and Fry (1971). Specimens morphologically identical to *U. ambloplitis* as described by Hunter (1933) should be sequenced for an adequate molecular and morphological comparison and a taxonomic conclusion regarding the form described by Dubois and Rausch (1948) and other previously synonymized species.

The overwhelming majority of ecological studies that report *Uvulifer* spp. did not include DNA sequence data (e. g., Boyd and Fry, 1971; Pérez-Ponce de León et al., 2010; Muzzall et al., 2011; McAllister et al., 2013; Flores-Lopes, 2014, Zimmermann et al., 2016; Hollander et al., 2019). Based on our results, it is clear that the diversity of *Uvulifer* in the New World is greater than previously recognized. At present, only 2 named species are currently known in North America north of Mexico (Boyd and Fry, 1971; López-Jiménez et al., 2018). Likely, many of the previous ecological studies dealing with larval stages of *Uvulifer* included more than a single *Uvulifer* species. Detailed molecular and morphological comparisons should provide a solution for this problem.

ACKNOWLEDGMENTS

We are grateful to Dr. John M. Bates (Field Museum, Chicago, Illinois), Tatiana Z. Pequeño Saco (Centro de Conservación, Investigación y Manejo de Áreas Naturales–Cordillera Azul), Dr. Eric Pulis (Northern State University, Aberdeen, South Dakota), Dr. Jason D. Weckstein (Drexel University, Philadelphia, Pennsylvania), Dr. Francisco Tiago de Melo (Federal University of Pará, Belém, Pará, Brazil), and Dr. João B. Pinho (Universidade Federal de Mato Grosso, Cuiabá, Mato Grosso, Brazil) for their invaluable help with field collecting. Collecting and processing of the specimens were supported by grant DEB-1120734 from the National Science Foundation and grant R15AI092622 from the National Institutes of Health, U.S.A., to V.V.T., and the Joe K. Neel Memorial Award from the University of North Dakota and Willis A. Reid, Jr. Student Research Grant from the American Society of Parasitologists to T.J.A.

LITERATURE CITED

Achatz, T. J., E. E. Pulis, K. Junker, T. T. Binh, S. D. Snyder, and V. V. Tkach. 2019. Molecular phylogeny of the Cyathocotylidae (Digenea, Diplostomoidea) necessitates systematic changes and reveals a history of host and environment switches. Zoologica Scripta 48: 545–556.

Blasco-Costa, I., and S. A. Locke. 2017. Life history, systematics and evolution of the Diplostomoidea Poirier, 1886: Progress, promises and challenges emerging from molecular studies. Advances in Parasitology 98: 167–225.

Boyd, E. M., and A. E. Fry. 1971. Metazoan parasites of the eastern belted kingfisher, *Megaceryle alcyon alcyon*. Journal of Parasitology 57: 150–156.

Caballero, E., and C. Diaz-Ungria. 1958. Intento de un catálogo de los tremátodos digéneos registrados en territorio Venezolano. Memoria de la Sociedad de Ciencias Naturales La Salle 18: 19–36.

Derycke, S., T. Remerie, A. Vierstraete, T. Backeljau, J. Vanfleteren, M. Vincx, and T. Moens. 2005. Mitochondrial DNA variation and cryptic speciation within the free-living marine nematode *Pellioditis marina*. Marine Ecology Progress Series 300: 91–103.

Dubois, G. 1938. Monographie des Strigeida (Trematoda). Mémoires de la Société Neuchâteloise des Sciences Naturelles 6: 1–535.

Dubois, G. 1964. Du statut de quelques Strigeata La Rue, 1926 (Trematoda). I. Bulletin de la Société Neuchâteloise des Sciences Naturelles 87: 27–71.

Dubois, G. 1985. Quelques Strigeoidea (Trematoda) récoltés chez des oiseaux du Paraguay par la Mission Claude Weber, automne 1983, du Muséum d'Histoire Naturelle de Genève. Revue Suisse de Zoologie 92: 641–648.

Dubois, G. 1988. Quelques Strigeoidea (Trematoda) récoltés au Paraguay par les expéditions du Muséum d'Histoire naturelle de Genève, au cours des années 1979, 1982 et 1985. Revue Suisse de Zoologie 95: 521–532.

Dubois, G., and R. Rausch. 1948. Seconde contribution a l'etude des strigeides (Trematoda) Nord-Américains. Bulletin de la Société Neuchâteloise des Sciences Naturelles 71: 29–61.

Dubois, G., and R. Rausch. 1950. A contribution to the study of North American strigeids (Trematoda). American Midland Naturalist 43: 1–31.

Flores-Lopes, F. 2014. The occurrence of black spot disease in *Astyanax* aff. *fasciatus* (Characiformes: Characidae) in the Guaíba Lake basin, RS, Brazil. Brazilian Journal of Biology 74: 127–134.

Hall, T. A. 1999. BioEdit: A user-friendly biological sequence alignment editor and analysis program for Windows 95/98/NT. Nucleic Acids Symposium Series 41: 95–98.

Hernández-Mena, D. I., M. García-Varela, and G. Pérez-Ponce de León. 2017. Filling the gaps in the classification of the Digenea Carus, 1863: Systematic position of the Proterodiplostomidae Dubois, 1936 within the superfamily Diplostomoidea Poirier, 1886, inferred from nuclear and mitochondrial DNA sequences. Systematic Parasitology 94: 833–848.

Hollander, C. A., B. N. Griffith, and M. R. Zimmermann. 2019. Differences in endohelminth parasite infection between male morphotypes of bluegill sunfish (*Lepomis macrochirus*). Journal of Parasitology 105: 135–142.

Hoogendoorn, C., N. J. Smit, and O. Kudlai. 2019. Molecular and morphological characterization of four diplostomid metacercariae infecting *Tilapia sparrmanii* (Perciformes: Cichlidae) in the North West Province, South Africa. Parasitology Research 118: 1–14.

Hunter III, G. W. 1933. The strigeid trematode, *Crassiphiala ambloplitis* (Hughes, 1927). Parasitology 25: 510–517.

Kudlai, O., A. Kostadinova, E. E. Pulis, and V. V. Tkach. 2015. A new species of *Drepanocephalus* Dietz, 1909 (Digenea: Echinostomatidae) from the double-crested cormorant *Phalacrocorax auritus* (Lesson) (Aves: Phalacrocoracidae) in North America. Systematic Parasitology 90: 221–230.

Kumar, S., G. Stecher, and K. Tamura. 2016. MEGA7: Molecular Evolutionary Genetics Analysis Version 7.0 for Bigger Datasets. Molecular Biology and Evolution 33: 1870–1874.

Larkin, M. A., G. Blackshields, N. P. Brown, R. Chenna, P. A. McGettigan, H. McWilliam, F. Valentin, I. M. Wallace, A. Wilm, R. Lopez, et al. 2007. Clustal W and Clustal X version 2.0. Bioinformatics 23: 2947–2948.

Locke, S. A., A. R. Van Dam, M. Caffara, H. A. Pinto, D. López-Hernández, and C. A. Blanar. 2018. Validity of the

Diplostomoidea and Diplostomida (Digenea, Platyhelminthes) upheld in phylogenomic analysis. International Journal for Parasitology 48: 1043–1059.

Lockyer, A. E., P. D. Olson, P. Østergaard, D. Rollinson, D. A. Johnston, S. W. Attwood, V. R. Southgate, P. Horak, S. D. Snyder, T. H. Le, et al. 2003. The phylogeny of the Schistosomatidae based on three genes with emphasis on the interrelationships of *Schistosoma* Weinland, 1858. Parasitology 126: 203–224.

López-Jiménez, A., G. Pérez-Ponce de León, and M. García-Varela. 2018. Molecular data reveal high diversity of *Uvulifer* (Trematoda: Diplostomidae) in Middle America, with the description of a new species. Journal of Helminthology 92: 725–739.

Lutz, H. L., V. V. Tkach, and J. D. Weckstein. 2017. Methods for specimen-based studies of avian symbionts. *In* The role of collections in ornithology: The extended specimen. Studies in avian biology, M. Webster (ed.). CRC Press, Boca Raton, Florida, p. 127–183.

McAllister, C. T., R. Tumlison, H. W. Robison, and S. E. Trauth. 2013. Initial survey on black-spot disease (Digenea: Strigeoidea: Diplostomidae) in select Arkansas fishes. Journal of the Arkansas Academy of Science 67: 200–203.

Muzzall, P. M., V. Cook, and D. J. Sweet. 2011. Helminths of belted kingfishers, *Megaceryle alcyon* Linnaeus, 1758, from a fish hatchery in Ohio, U.S.A. Comparative Parasitology 78: 367–372.

Niewiadomska, K. 2002. Family Diplostomidae Poirier, 1886. *In* Keys to the Trematoda, vol. 1, D. I. Gibson, A. Jones, and R. A. Bray (eds). CAB International and Natural History Museum, London, U.K., p. 167–196.

Pérez-Ponce de León, G., and D. Hernández-Mena. 2019. Testing the higher-level phylogenetic classification of Digenea (Platyhelminthes, Trematoda) based on nuclear rDNA sequences before entering the age of the 'next-generation' Tree of Life. Journal of Helminthology 93: 260–276.

Pérez-Ponce de León, G., R. Rosas-Valdez, R. Aguilar-Aguilar, B. Mendoza-Garfias, C. Mendoza-Palmero, L. García-Prieto, A. Rojas-Sánchez, R. Briosio-Aguilar, R. Pérez-Rodríguez, and O. Domínguez-Domínguez. 2010. Helminth parasites of freshwater fishes, Nazas River basin, northern Mexico. Check List 6: 26–35.

Rambaut, A. 2016. Figtree (version 1.4.3). Available at: http://tree.bio.ed.ac.uk/software/figtree/. Accessed 14 March 2019.

Remsen Jr., J. V. 1991. Community ecology of Neotropical kingfishers. University of California Publications in Zoology 124: 1–128.

Ronquist, F., and J. P. Huelsenbeck. 2003. MRBAYES 3: Bayesian phylogenetic inference under mixed models. Bioinformatics 19: 1572–1574.

Stoyanov, B., S. Georgieva, P. Pankov, O. Kudlai, A. Kostadinova, and B. B. Georgiev. 2017. Morphology and molecules reveal the alien *Posthodiplostomum centrarchi* Hoffman, 1958 as the third species of *Posthodiplostomum* Dubois, 1936 (Digenea: Diplostomidae) in Europe. Systematic Parasitology 94: 1–20.

Subair, K. T., R. Brinesh, and K. P. Janardanan. 2013. Studies on the life-cycle of *Uvulifer iruvettiensis* sp. nov. (Digenea: Diplostomidae). Acta Parasitologica 58: 91–97.

Tkach, V. V., and S. S. Curran. 2015. *Prosthenystera oonastica* n. sp. (Digenea: Callodistomidae) from ictalurid catfishes in southeastern United States and molecular evidence differentiating species in the genus across Americas. Systematic Parasitology 90: 39–51.

Tkach, V. V., D. T. J. Littlewood, P. D. Olson, J. M. Kinsella, and Z. Swiderski. 2003. Molecular phylogenetic analysis of the Microphalloidea Ward, 1901 (Trematoda: Digenea). Systematic Parasitology 56: 1–15.

Tkach, V. V., and J. Pawlowski. 1999. A new method of DNA extraction from the ethanol-fixed parasitic worms. Acta Parasitologica 44: 147–148.

Van Steenkiste, N., S. A. Locke, M. Castelin, D. J. Marcogliese, and C. Abbott. 2015. New primers for DNA barcoding of digeneans and cestodes (Platyhelminthes). Molecular Ecology Resources 15: 945–952.

Yamaguti, S. 1971. Synopsis of the digenetic trematodes of vertebrates. Vols. 1 and II. Keigaku Publishing, Tokyo, Japan, 1,074 p.

Zimmermann, M. R., K. E. Luth, and G. W. Esch. 2016. Transmission pattern differences of miracidia and cercariae larval stages of digenetic trematode parasites. Acta Parasitologica 61: 680–688.